IRAM Newsletter

Number 21 May 12, 1995

Calendar

Executive Council: June 28/29, 1995

Observing proposals: Proposals for the period *Nov 15, 1995 to May. 15, 1996* should be submitted before *September 4th, 1995*

Contents

30m Telescope

Successful 19–channel Bolometer Period in March/April 1995

In the past winter period, the MPIFR 7–channel bolometer and later, after a technical and scientific verification phase, also the MPIFR 19–channel bolometer, were offered to the astronomical community, the latter one for the first time. It was installed and tested by the MPIfR bolometer group and IRAM during the second week in March and was then available for observations until the beginning of April.

A plot of the 1.3mm zenith optical depth during the bolometer period is shown in Fig. 1. Except at the beginning of the observing period, where observations were impossible due to weather, the instrument could be used most of the time (with only a few interruptions due to small technical problems). Due to the increased data rate, the computer system was pushed to the limit. Improvements are foreseen for the future.

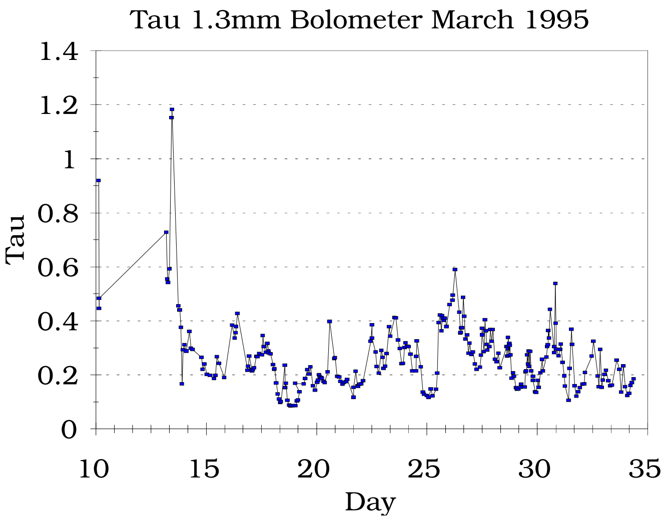

Figure 1: Zenith optical depth at 1.3 mm during March and beginning of April 1995

The bolometer was mainly used in on–the–fly mapping mode, where one gained a factor 2 or more in observing time compared to the 7–channel Bolometer. A single coverage resulted in a map with RMS noise typically between 6 and 12 mJy/beam. A report on test results from the 19-channel bolometer will be given in a future copy of the Newsletter.

Conversion of source velocity/redshift to sky frequency

Sometimes confusion may arise on how to calculate the sky frequency for a given redshift or source velocity. This stems from the fact that optical and radio astronomers calculate radial source velocities from different formulas. (Remember that velocities are not directly measured but calculated from wavelength or frequency shifts). Optical astronomers deduce radial velocities from the measurement of a wavelength shift:

$$v_{\rm opt} = c\,z = c\,\frac{\lambda - \lambda_o}{\lambda_o}\ \left(= c\,\frac{f - f_0}{f}\right), \qquad (1)$$

where c is the speed of light, λ_o (f_0) the unshifted and λ (f) the shifted wavelength (frequency), respectively. The astronomical redshift z is defined as

$$z = \frac{\lambda - \lambda_o}{\lambda_o}. \tag{2}$$

At low redshifts some radio astronomers use a different convention which presumably comes from the fact that frequency shifts rather than wavelength shifts are measured. The radio convention is

$$v_{\rm radio} = c\,\frac{f_0 - f}{f_0}\,\left(= c\,\frac{\lambda - \lambda_o}{\lambda}\right) \neq cz. \tag{3}$$

As a consequence, radio "velocity" and optical recession velocity are not the same for a given redshift:

$$v_{\rm opt} \neq v_{\rm radio}. \tag{4}$$

This means that in order to calculate the correct sky frequency from a given velocity one needs to know if the velocity was calculated using the optical or radio convention. An optical velocity $v_{\rm opt}$ (or redshift z) requires another formula than a radio velocity $v_{\rm radio}$ obtained *e.g.* from 21 cm HI measurements. The sky frequency $f_{\rm sky}$ for a given source velocity and line rest frequency f_0 is

– optical convention:

$$f_{\rm sky} = f_0\,\frac{1}{1+z} = f_0\,\frac{1}{1+v_{\rm opt}/c}$$

– radio convention:

$$f_{\rm sky} = f_0\,(1 - \frac{v_{\rm radio}}{c})$$

For a given velocity the sky frequencies calculated with the two formulas above can differ significantly. For example, calculating the sky frequency in the 230 GHz range with the inappropriate formula (optical instead of radio convention, or vice versa) at a source velocity of 10000 km/sec results in an error of about 250 MHz. At 20000 km/sec, this error has increased to about 1 GHz!

At the IRAM 30m telescope the conversion is done in the following way: the drive program calculates the velocity $v_{\rm lsr}^{\rm tel}$ of the telescope relative to the local standard of rest, takes the source velocity $v_{\rm lsr}^{\rm source}$ (from the source catalogue), and then calculates the sky frequency applying the optical convention:

$$\begin{aligned} v_{\rm opt} &= v_{\rm lsr}^{\rm tel} + v_{\rm lsr}^{\rm source} & (5)\\ f_{\rm sky} &= f_0\,\frac{1}{1+v_{\rm opt}/c}. & (6) \end{aligned}$$

If you want to observe *e.g.* a high-redshift object with redshift z at line rest frequency f_0, the *recommended procedure* is to set the source velocity v (in the source catalogue) to zero and give the corrected frequency (calculated with the optical formula) $f_0' = f_0[1/(1+z)]$ to the drive program by using the OBS command:

`RECEIVER` *rx_name* `/FREQUENCY` f_0' `LSB` .

You might alternatively calculate the optical source velocity $v_{\rm opt} = c\,z$, give this velocity in the source catalogue, and use the line rest frequency f_0 in the OBS command:

`RECEIVER` *rx_name* `/FREQUENCY` f_0 `LSB` .

If you need to use the radio convention, it is best to set the source velocity v (in the source catalogue) to zero and give the corrected frequency (calculated with the radio formula) $f_0' = f_0(1 - v_{\rm radio}/c)$ using the OBS command:

`RECEIVER` *rx_name* `/FREQUENCY` f_0' `LSB`

instead of the line rest frequency.

Instead of giving frequencies directly in the `RECEIVER` command, you can also define a line with the corrected frequency in your line catalogue, and use the OBS command:

`RECEIVER` *rx_name* `/LINE` *your_line*.

Wolfgang WILD

Interferometer

230 GHz fringes

On April 3, a major upgrade was started on Plateau de Bure, which included a complete change of the LO distribution system, continuum detectors, and the replacement of 2 "old" 3-mm SIS receivers by dual-frequency systems covering the the 3mm and 1.3mm bands on antennas 1 and 2. These improvements had major consequences on the control software, since the new hardware (receiver and LO system) is entirely controlled by VME micro-processors linked to the central computer by Ethernet.

After less than 2 weeks of intense activity, the array was back into operation at 3mm and the first 1.3mm tests were performed. First fringes at 230 GHz were actually obtained on April 12, at 12:15 on 3C84, between antenna 1 and 4 (Figure 2), but effectively "seen" only a week later because low signal to noise prevented immediate identification and other urgent tests needed to be performed.

On April 18, just before a bad weather period, fringes were again obtained at 230 GHz between antenna 1 and 4 on several sources: 3C273, 3C279, NRAO530 and 3C345. Higher signal to noise allowed immediate checks of pointing and focus differences between the 3 mm and 1.3 mm receiver. The baseline length was 160 m, which corresponds to the highest spatial resolution ever used at Plateau de Bure. Because of the poor weather conditions and long baselines, phase stability was bad (even at 3mm), but there is an excellent correlation between the 3mm and 1.3 mm phases and even between the phases and the total power output of the 1.3 mm receivers (See "Phase correction" section, page 5).

The new receivers have typical receiver noise temperatures of about 45 K in the 3mm band (with a rejection of 6 dB of the image sideband), and 50 K in the 1.3mm band (210 to 250 GHz).

Final software modifications were carried out between April 23 and April 26, and the Plateau de Bure interferometer was fully back into normal operation on April 26.

Program committee recommendations

The following table shows the recommendations of the program committee for the scheduling period May 15, 1995, to November 15, 1995:

Project	Rate	Project	Rate	Project	Rate
E031	A	E039	A	E043	A
E045	A	E057	A	E008	A
E034	B	E049	B	F001	C
F002	C	F003	C	F004	A
F005	C	F006	A	F007	B
F008	B	F009	A	F010	B
F011	A	F012	A	F013	A
F014	B	F015	A	F016	C
F017	C	F018	C	F019	A
F020	C	F021	C	F022	B
F023	A	F024	A	F025	A
F026	B	F027	C	F028	B

(*Project Status*: A: Accepted, B: Backup if time available, C: Rejected.)

In the above table, the first five A projects are backup proposals from the last observing session which have been started recently.

The A programs will be scheduled in priority. Further time, if it becomes available, will go to the B programs, taking into account scientific merit, crowding in certain right ascension ranges and general aspects of balance. B proposals will only be started in case of available observing time. Some B proposals will be carried out with 3 antennas during the summer maintenance period (June-July). Note that B projects which cannot be started will no longer be automatically resubmitted: authors have to resubmit them explicitly.

observations

The following projects have been completed:

C061	D032	D039	D072	E005	E012
E014	E028	E033	E035	E037	E041
E044	E048	E054	E056	E059	E062
E063	E064	E075			

The status of on-going projects (which includes some of the newly accepted projects) is the following:

Project	Done	Remaining	Total
E031	C2	C1 D	CD
E039	D C1 C2	B1 B2	BCD
E040		B1 B2	B (backup)
E043	c1c, C2	(C1) B1 B2	BC
E045	C1, C2	B1 B2	BC
E057	C1, C2	B1 B2	BC
E076	C2		3-ant
F004	(C2)	C1 (C2) D	CD
F009		C1 C2 D	CD
F023		C1 C2 D	CD
F024		Any	Detection
F025		C1 C2 D	CD

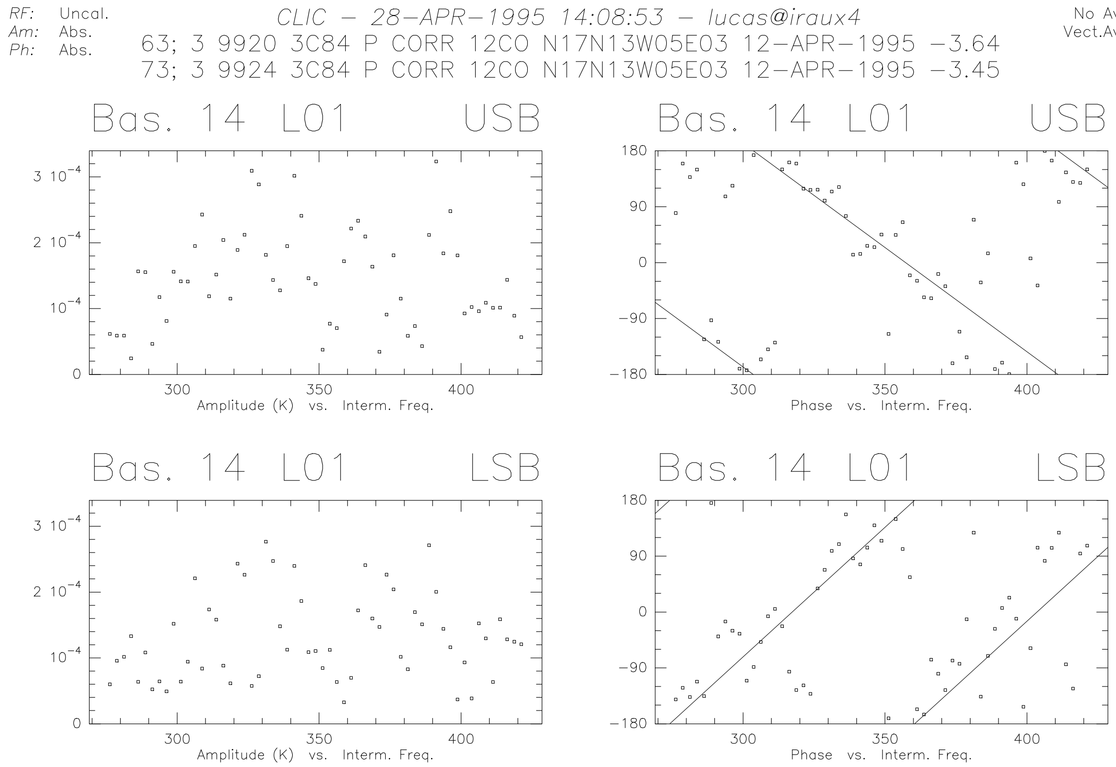

Figure 2: First 1.3mm fringes on April 12. An uncorrected 10ns delay offset causes the strong frequency dependence of the phases.

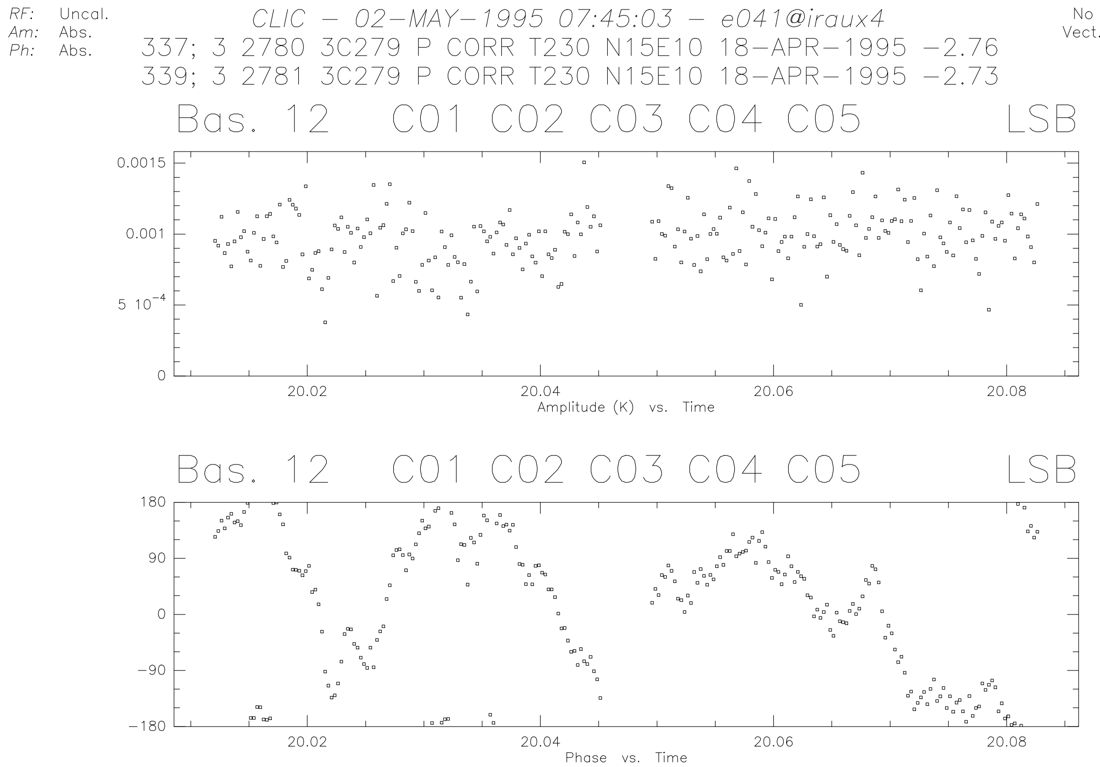

Figure 3: 1.3mm observed on April 18, from 3C279, on a 160m baseline: Amplitude and phase as a function of time.

Note that the long baseline observations may be difficult to perform for two reasons: 1) we are approaching the summer conditions 2) ground work is required near station N20 for the North/South baseline extension this summer.

Stéphane GUILLOTEAU

Phase correction with the dual frequency receivers

With the installation of the two new dual frequency receivers, it became possible to study the correlation between the total power fluctuations at 230 GHz and the phase noise induced by atmospheric water vapor. This is an important step to extend the total amount of available observing time, because the performance of the interferometer in general and especially at longer baselines and higher frequencies depends critically on the variations of water vapor along the line of sight, which is one of the least stable constituents of the atmosphere (with time scales down to a few seconds). Due to its spectral lines in the infrared, the water molecule changes its optical properties when moving from the visible range to mm wavelengths, notably the refractive index. That means that a "clear sky" in human terms is in fact filled with refracting bubbles with sizes from some kilometers down to less than a meter for the PdB Interferometer. During summer, the available observing time is mainly limited by the abundance of the turbulence cells above the telescopes.

Various phase correction schemes are under development at other interferometers (ATNF, Nobeyama, VLA, BIMA, and others) that partly rely on dedicated radiometers for remote atmospheric sounding because of the stringent stability requirements for the receivers. At IRAM, the previous mixer generation was not sufficiently stable to isolate the atmospheric component from the total power fluctuations, but the new receivers showed promise that the necessary requirements could be met. The dual frequency capabilities would allow to use the spectral region around 230 GHz for the water vapor estimation which shows a sensitivity about six times higher (Bremer 1994) than the 22.2 GHz line monitored in conventional radiometers (Moran and Rosen 1981, Elgered, Rönnäng and Askne 1980) and to correct the phase at both frequencies in real time.

In the evening of April 18, antennas 1 and 4 observed the quasar 3C279 (a strong source regularly used as phase calibrator) at 86 and 230 GHz simultaneously on a baseline of 160.5 m. Adjustments of the hardware were still in progress, so the data is not calibrated. Figure 4 shows the variations of amplitude and phase at 86 GHz with time, the "raw" difference in the total powers TP of antennas 1 and 4 at 230 GHz, and a fit of the form

$$\phi_{\rm atm} = a \cdot TP(1) + b \cdot TP(2) + c \cdot time + d \qquad (7)$$

to the phase, which allows for a linear drift in time. After the subtraction of a linear slope, the uncorrected phase shows a mean deviation of 49.4°, whereas the corrected phase shows a mean deviation of 11.8°. Approximating the atmospheric phase shifts with a Gaussian random variable of mean deviation σ (Thompson 1986), one can describe their influence on the visibilities V as

$$\langle V_{\rm measured} \rangle = V_{\rm true} \cdot \exp\left(-\frac{\sigma^2}{2}\right) \qquad (8)$$

With the reduction of the noise, the sensitivity of the interferometer has therefore been improved by a factor of 1.44. The true improvement is however even greater in our case, since phase calibration would be only marginally possible with a phase rms of $\sim 50°$, while it should be easy with a rms of $\sim 12°$.

Although these results are encouraging, it will be necessary to do more testing under different atmospheric conditions before real time phase correction can be offered on a regular basis. Especially in the presence of clouds, the calibration factor between phase and total power fluctuations is supposed to change dramatically which could cause a counterproductive correction.

Further observations will also test the validity of the phase correction when the interferometer is switched between nearby phase calibrators.

References:

Bremer M. 1994, The Phase Project: First Results, IRAM internal report

Moran J.M., Rosen B.R. 1981, Radio Science Vol. 16 No. 2, pp. 235-244

Elgered G., Rönnäng B.O., Askne J.I.H. 1980, Research Report No. 141, Chalmers University of Technology, Gothenburg, Sweden

Thompson A.R. 1986, Interferometry and Synthesis in Radio Astronomy, Wiley & Sons

Michael BREMER, Stéphane GUILLOTEAU, Robert LUCAS

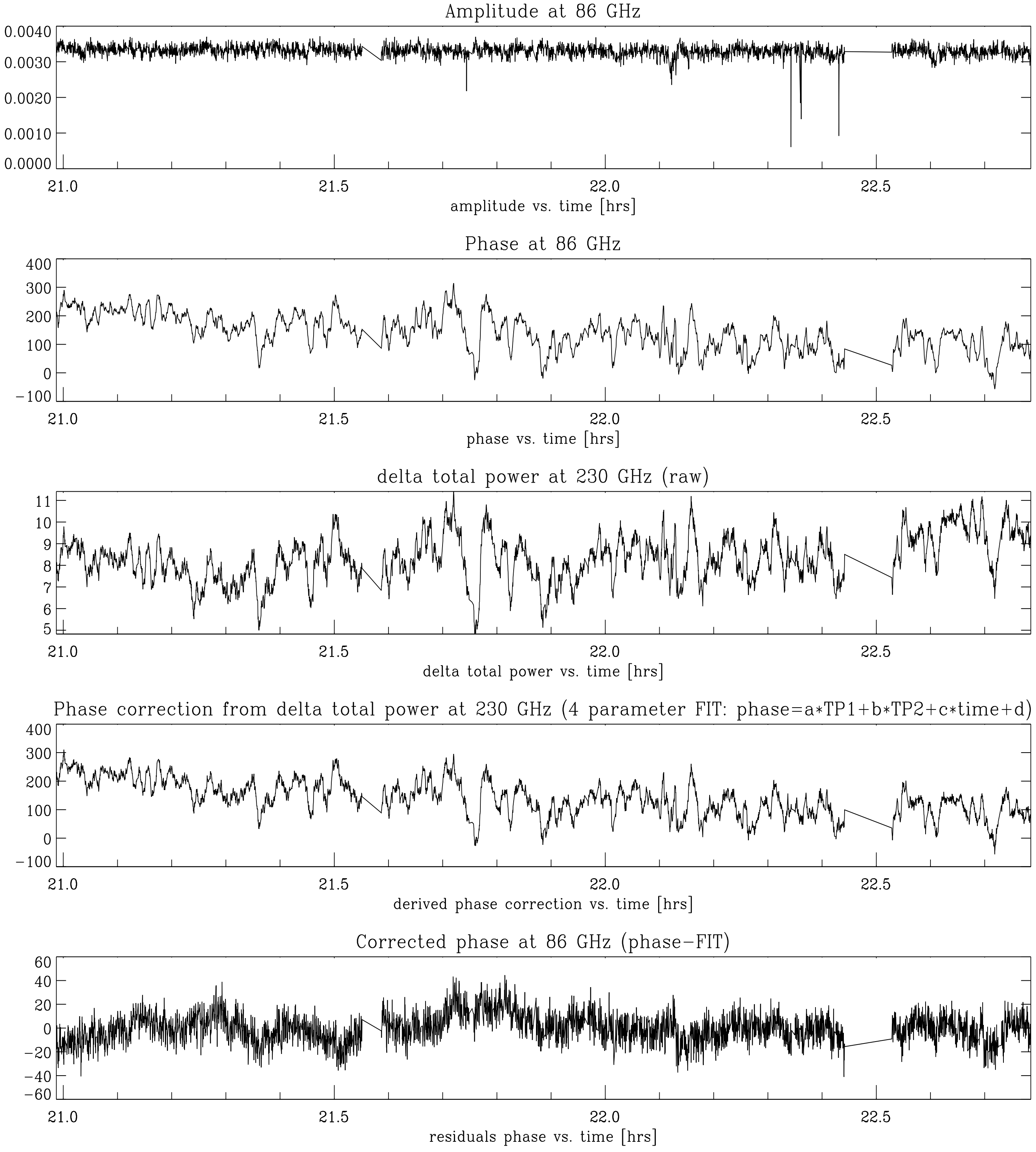

Figure 4: Observation of 3C279 on April 18 with antennas 1 and 4 on a baseline of 160.5 m. Fit parameters were $a = 47.6, b = -56.2, c = -100.6, d = 3238$ (cf. equ. 7).

Scientific Results

Methanol enhancement in young bipolar outflows

R. Bachiller[1], S. Liechti[1], C.M. Walmsley[2], and F. Colomer[1]
[1] Centro Astronómico de Yebes, Apartado 148, E-19080 Guadalajara, Spain
[2] Physikalisches Institut, Universität zu Köln, Zulpicherstr. 77, D-50937 Köln, Germany

Abstract: We report observations of the 2_k–1_k, 3_k–2_k, and 5_k–4_k thermal lines of CH_3OH toward young bipolar outflows. Strong emission ($\gtrsim$ 6 K, in the case of L 1157) is observed toward the shocked molecular regions associated with the lobes of some outflows, whereas the emission from the cold quiescent material in the surrounding molecular core is rather weak ($\lesssim$ 1 K). We have derived the methanol abundance by combining the CH_3OH data with new $C^{18}O$ observations. It results that methanol is enhanced by large factors toward the shocked regions ($\sim$ 400 toward the blue-shifted lobe of L 1157). Although the shocked gas is known to be heated to about 100 K, the CH_3OH rotation temperatures have moderate values: in L 1157 $T_{\rm rot}$ increases from 8 K in the ambient gas to 12 K in the shocked region. Radiative transfer calculations, carried out to simulate the CH_3OH excitation in different physical circumstances, confirm that in the range of physical conditions discussed here the methanol molecules are very subthermally excited, and $T_{\rm rot}$ is not a good measure of the kinetic temperature ($T_{\rm rot} << T_{\rm K}$). The observed methanol abundance enhancements are likely caused by processes of desorption of grain mantles in shocks.

An extremely-high-velocity multipolar outflow around IRAS 20050+2720

R. Bachiller[1], A. Fuente[1] and M. Tafalla[2]
[1] Centro Astronómico de Yebes (OAN, IGN), Apartado 148, E-19080 Guadalajara, Spain
[2] Harvard-Smithsonian Center for Astrophysics, MS 42, 60 Garden Street, Cambridge, MA 02138, USA

Abstract:

We report high-angular resolution maps in the CO 2$\rightarrow$1 and CS 3$\rightarrow$2 lines of the molecular gas around the embedded object IRAS 20050+2027 (figure reffig:bachiller). This is a 260 $L_\odot$ source located in the Cygnus Rift at 700 pc from the Sun. The CS data uncover a dense core of size 0.3 pc, and 80 $M_\odot$ centered on the IRAS object. The CO map reveals a remarkable molecular outflow consisting of three pairs of lobes emanating from the close vicinity of the IRAS source. One of the lobe pairs is a highly-collimated jet of extremely high-velocity emission (LSR velocities up to $\pm$70 km/s) containing molecular "bullets".

We briefly examine different possibilities to explain the complex structure of the multipolar outflow. A single outflow appears unable to explain all the CO observations, so we suggest that two or three independent outflows emanate from different young sources embedded within the core.

Cold dust emission from the spiral arms of M 51

M. Guélin([1]), R. Zylka([2]), P.G. Mezger([2]), C.G.T. Haslam([2]), E. Kreysa([2])
([1])IRAM, 300 rue de la piscine, F-38406 S$^{\rm t}$ Martin d'Hères, France
([2])Max Planck Institut für Radioastronomie, Auf dem Hügel 69, D-53121 Bonn 1, Germany

Abstract: Using the IRAM 30-m telescope equipped with the MPIfR 7-channel bolometer array, we have mapped the λ 1.2 mm continuum emission of the inner part of M 51 (Fig. 6). This emission traces the central molecular disk and the inner spiral arms and correlates remarkably well with the ^{12}CO (2–1) line emission. The λ 1.2 mm continuum to CO line intensity ratio, averaged over the 70 GHz-wide bolometer band, is 7; a similar value was derived for NGC 891.

The λ 1.2 mm emission arises mostly from cold dust ($T_d \leq$ 20 K) associated with molecular clouds. Using the local Galactic value of the dust absorption cross section, corrected for the larger metallicity observed near M 51's center, we derive the gas distribution from this emission. The derived molecular masses are $\simeq$ 4 times smaller than those obtained from the CO luminosity, using Strong et al.'s Galactic CO to H_2 conversion factor ($X = N_{\rm H_2}/I({\rm CO}) = 2.3\ 10^{20}{\rm mol.cm^{-2}K^{-1}km^{-1}s}$), but close to the masses estimated from ^{13}CO and from visual extinction.

It may be argued, considering the crude approximations inherent to each method, that all estimates are encouragingly close. We wish to stress, however, that the present work points towards an H_2 mass in the inner part of M 51 *a factor of 4 lower* than usually assumed from the ^{12}CO integrated line intensity. A similar conclusion was reached for NGC 891 (Guélin et al. 1995, A&A 279, L37). It probably also applies to many galaxies and could have major consequences on their evolution.

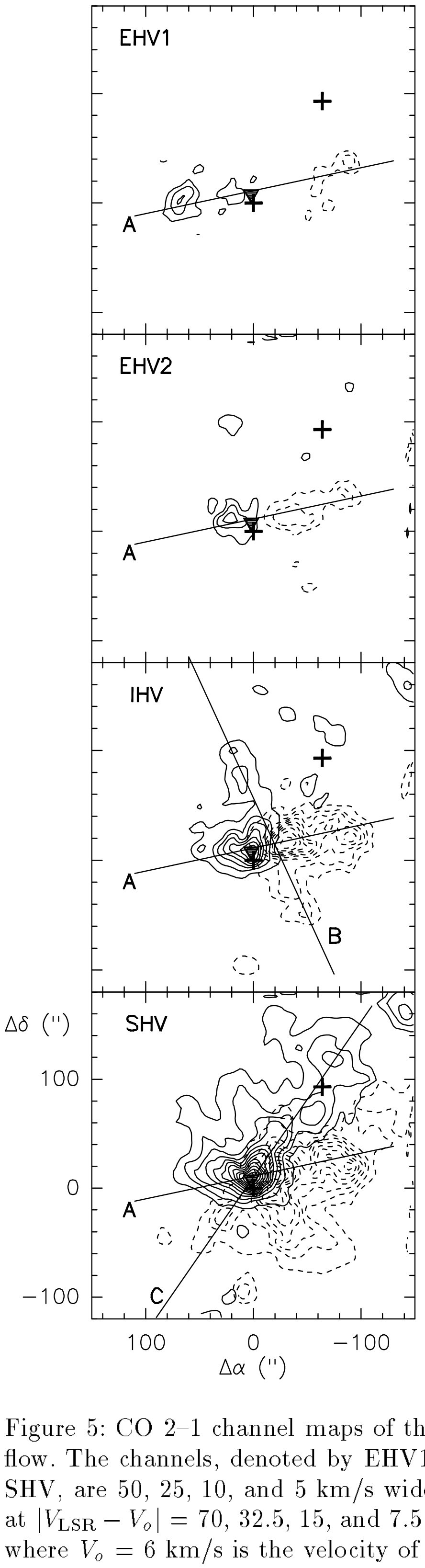

Figure 5: CO 2–1 channel maps of the IRAS 20050 outflow. The channels, denoted by EHV1, EHV2, IHV, and SHV, are 50, 25, 10, and 5 km/s wide, and are centered at $|V_{\rm LSR} - V_o| = 70$, 32.5, 15, and 7.5 km/s, respectively, where $V_o = 6$ km/s is the velocity of the ambient cloud. First contour and step are at 10 K km/s for the EHV intervals, and 7 K km/s for the SHV and IHV intervals. Solid contours are for the blue-shifted emission, and dashed contours for the red-shifted. The origin is at the nominal position of IRAS 20050. The crosses represent the IRAS sources IRAS 20050 and IRAS 20049+2721, and the triangle marks the position of a strong CS emission peak. The axes A, B, C are drawn to illustrate the multi-lobe structure of the outflow.

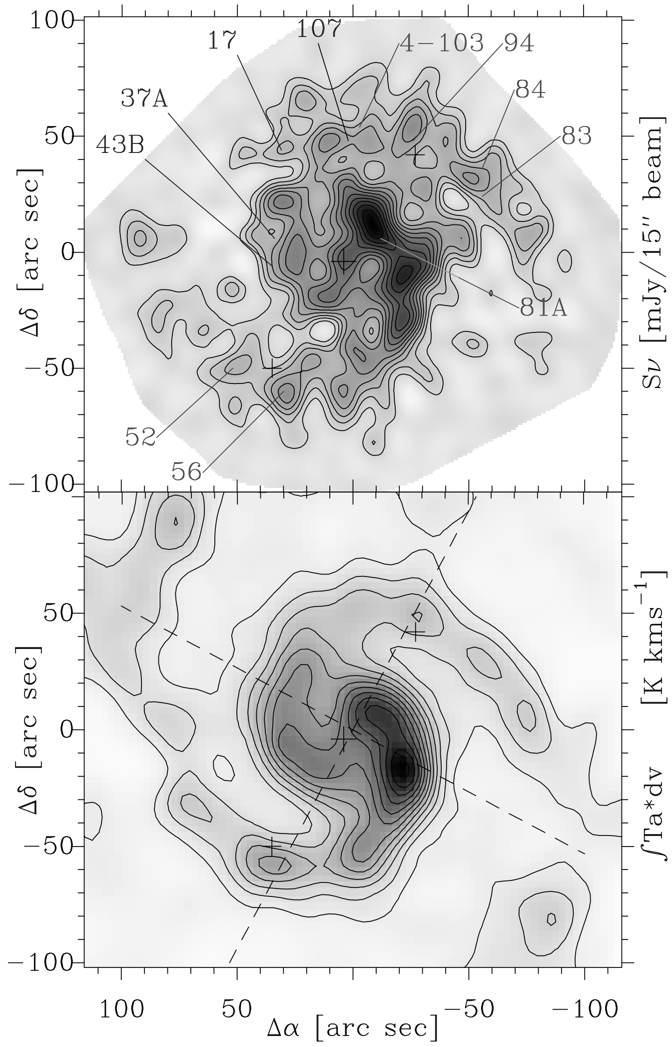

Figure 6: The λ 1.2 mm continuum emission (S_ν —*top*) and the velocity integrated CO line intensity ($I(^{12}\mathrm{CO})$ — *bottom*) in the inner part of M 51, smoothed to a 15″ angular resolution. The position of selected Hα regions are indicated on the continuum map (numbering according to Carranza et al. A&A 1, 479). Contour levels range from $S_\nu = 10$ to 46 mJy (beam)$^{-1}$ in steps of 3 mJy.(beam)$^{-1}$ for the continuum, and from $I(^{12}\mathrm{CO}) = 5$ K.km^{-1}s to 32.5 K.km^{-1}s in steps of 2.5 K.km^{-1}s for CO. The continuum emission was set to zero outside the diamond-shaped grey area. Both maps were observed with the IRAM 30-m telescope; the CO data are taken from Garcia-Burillo et al. (1993, A&A 274, 123).

New Preprints

The following preprints are available from IRAM:

353. Methanol enhancement in young bipolar outflows
R. Bachiller, S. Liechti, C.M. Walmsley, F. Colomer
1995 *Astron. and Astrophys.*

354. Ammonia emission from bow shocks in the L1157 outflow
M. Tafalla, R. Bachiller
1995 *Astrophys. Journal*

355. High density CN filaments in NGC 2023
A. Fuente, J. Martin-Pintado, R. Gaume
1995 *ApJ. Letters*

356. An extremely high velocity multipolar outflow around IRAS 20050+2720
R. Bachiller, A. Fuente, M. Tafalla
1995 *Ap.J. Letters*

357. A 3d iterative deprojection technique
M. Bremer
1995 *A & A Supplement Series*

New Working Report available:

228/95 Frequency switching at the 30m telescope
C. Thum, A. Sievers, S. Navarro, W. Brunswig, J. Peñalver

The IRAM Newsletter is edited by Robert LUCAS at IRAM-Grenoble (e-mail address: `lucas@iram.fr`).

The IRAM Newsletter is available in electronic form:

- by using the World Wide Web and NCSA Mosaic: from the IRAM home page (`http://iram.fr/www/iram.html`), click on item "Newsletter" and follow the links...
- by means of an anonymous `ftp` account, opened at IRAM for Internet users. To access those files, please connect through `ftp` to `iraux2.iram.fr` (or `193.48.252.22`) and read the `README` file. Several subdirectories are available:

Directory	Contents
`/dist/newsletter`	Recent issues of this Newsletter (one subdirectory per issue)
e.g. `/dist/newsletter/may94`	may94.ps is the Postscript file for the january 1994 issue.
`/dist/doc`	Documentation on IRAM telescopes and software
`/dist/proposal`	Proposal forms and Latex files to aid proposal preparation
`/dist/soft`	distribution files for reduction software

- by means of an electronic mail file server installed at IRAM (on the VAX machine IRAM04). This file server is a file distribution service that uses electronic mail facilities to deliver files. To communicate with it you should send a message to the electronic address:

  `newsserv@iram.grenet.fr`

  For instance, to obtain a copy of the May 1992 issue, just send the one line message:

  `SENDME MAY92.PS`

  to the above electronic address. You will receive later a mail message containing the IRAM Newsletter in Postscript code. Please discard all the e-mail header information with a text editor, and send the file to a Postscript laser printer.

  More information may be obtained by sending the one line message:

  `HELP`

  Note that this file server also contains Postcript files of the proposal forms and of Plateau de Bure documentation.

We also compile a list of e-mail addresses of IRAM users (e.g., in order to send warning messages when the Newsletter is available, but also to provide fast information, if needed). If you feel your address should be on this list, please send the one line message:

`SUBSCRIBE`

to the following e-mail address:

`iramusers-request@iram.grenet.fr`

Both addresses are valid on Internet, EARN-Bitnet and EAN .... Please keep R. Lucas informed of any problem you may encounter.

IRAM Addresses:

	Address:	Telephone:	Fax:
Grenoble	Institut de Radioastronomie Millimétrique, 300 rue de la Piscine, Domaine Universitaire, 38406 St Martin d'Hères Cedex, France	(33) 76 82 49 00	(33) 76 51 59 38
Plateau de Bure	Institut de Radioastronomie Millimétrique, Observatoire du Plateau de Bure, 05250 St Etienne en Dévoluy, France	(33) 92 52 53 60	(33) 92 52 53 61
Granada	Instituto de Radioastronomía Milimétrica, Avenida Divina Pastora 7, Núcleo Central, 18012 Granada, España	(34) 58 27 95 08	(34) 58 20 76 62
Pico Veleta	Instituto de Radioastronomía Milimétrica, Estación Radioastronómica IRAM-IGN del Pico Veleta, Sierra Nevada, 18012 Granada, España	(34) 58 48 02 11	(34) 58 48 08 60

E-Mail Addresses:

- IRAM-Grenoble: `username@iram.fr`, or through PSI: `PSI%0208038080590::username`
- IRAM-Granada: `username@iram.es`, or through SPAN: `IRAMEG::username` or `16494::username` or through PSI: `PSI%02145258020628::username`

The `username` is generally the last name of the person to be contacted.